Optimizing Charge Switching in Membrane Lytic Peptides for Endosomal Release of Biomacromolecules.

AUTHOR(S):

Sakamoto, Kentarou; Akishiba, Misao; Iwata, Takahiro; Murata, Kazuya; Mizuno, Seiya; Kawano, Kenichi; Imanishi, Miki; Sugiyama, Fumihiro; Futaki, Shiroh

CITATION:

Sakamoto, Kentarou ...[et al]. Optimizing Charge Switching in Membrane Lytic Peptides for Endosomal Release of Biomacromolecules.. Angewandte Chemie International Edition 2020, 59(45): 19990-19998

ISSUE DATE:

2020-11-02

URL:

http://hdl.handle.net/2433/261198

WILEY-VCH

RESEARCH ARTICLE

Optimizing charge switching in membrane lytic peptides for endosomal release of biomacromolecules

Kentarou Sakamoto,[a] Misao Akishiba,[a] Takahiro Iwata,[a] Kazuya Murata,[b] Seiya Mizuno,[b] Kenichi Kawano,[a] Miki Imanishi,[a] Fumihiro Sugiyama,[b] and Shiroh Futaki[a]*

[a] K. Sakamoto, Dr. M. Akishiba, T. Iwata, Dr. K. Kawano, Dr. M. Imanishi, Prof. Dr. S. Futaki
Institute for Chemical Research
Kyoto University, Gokasho, Uji, Kyoto 611-0011 (Japan)
E-mail: futaki@scl.kyoto-u.ac.jp
[b] Dr. K. Murata, Dr. S. Mizuno, Prof. Dr. F. Sugiyama
Laboratory Animal Resource Center, Transborder Medical Research Center, Faculty of Medicine, University of Tsukuba
Tennodai 1-1-1, Tsukuba, Ibaraki 305-8575 (Japan)

Supporting information for this article is given via a link at the end of the document.

Abstract: Endocytic pathways are practical routes for the intracellular delivery of biomacromolecules. Along with this, effective strategies for endosomal cargo release into cytosol are desired to achieve successful delivery. Focused on compositional differences between the cell and endosomal membranes and the pH decrease within endosomes, we designed the lipid-sensitive and pH-responsive endosome lytic peptide HAad. This peptide contains aminoadipic acid (Aad) residues, which serve as a safety-catch for preferential permeabilization of endosomal membranes over cell membranes, and His-to-Ala substitutions to enhance the endosomolytic activity. The ability of HAad to destabilize endosomal membranes was also supported by the model studies using large unilamellar vesicles (LUVs) and by increased intracellular delivery of biomacromolecules (including antibodies) into live cells. Cerebral ventricle injection of Cre recombinase with HAad led to Cre/loxP recombination in a mouse model, showing potential applicability of HAad in vivo.

Introduction

Biopharmaceutical proteins, including antibodies, have a profound therapeutic impact when delivered into the cell interior.[1-3] The delivery approaches of chemically modified peptides and proteins should also be of valuable tools for chemical biology studies analyzing and modulating molecular interplay in cells. However, the cell membrane (plasma membrane) works as a barrier to protect cells, which prevents permeation of hydrophilic macromolecules, including proteins, through cell membranes. Endocytic pathways, cellular uptake mechanism of extracellular substances, have been employed as an alternative route to deliver exogenous molecules into cell interiors. Endocytosis is a cellular vesicular transport system. Endocytosed molecules have to be released from endosomes into the cytosol (i.e., endosomal escape) to obtain their expected activities.[4-12] Although numerous approaches have been developed to stimulate endosomal escape, there has been considerable room to improve the efficacy.

To establish endosomal escape, the permeabilization of the endosomal membrane is needed. However, this may also be accompanied by the rupture of other membranes, including cell membranes, which will bring damages to cells. Therefore, switching mechanisms in the mode of membrane permeabilization between these membranes are needed. A typical approach is to utilize pH differences between inside endosomes (pH ~5) and outside the cells (pH ~7). Endosomal maturation is accompanied by a decrease in pH within endosomes. A variety of pH-sensitive membrane lytic peptides and polymers have thus been developed. One of the most typical approaches is to employ carboxylates as for adjusting the permeabilization activity. The carboxy group is in a charged form at extracellular, neutral pH, but it becomes protonated and non-charged at acidic pH. Insertion of Glu in membrane lytic peptides/polymers may lead to attenuation of the hydrophobic interaction to cell membranes and thus lytic activity on cell surfaces. Possible protonation of Glu at endosomal pH diminishes the hydrophilicity of the peptides/polymers, leading to an increase in their interaction to membranes to lyse the endosomal membranes. However, the pH inside endosomes has been considered to be 5 or so, where a certain percentage of carboxy moiety (p*K*a, 4.07) should remain in its charged state, and this prevents from exerting its wild type activity. Not only more effective pH-dependent charge-switch but also new design standpoints are necessary to stimulate better endosomal escape.

This study employed net positive amphiphilic peptides, endowed them both pH and lipid-charge responsive lytic activity, and established a delivery system capable of delivering bioactive proteins, including antibodies into the cell interior. We used L17E (IWLTALKFLGKHAAKHEAKQQLSKL-amide, Figure 1, and Figure 2B), which is a lytic peptide bearing net positive charges developed by our group as a template.[13] Marked intracellular delivery of various proteins, including antibodies (immunoglobulin G, IgG) was attained by the addition of this peptide in the incubation media. However, mechanistic studies revealed that the endosomolytic activity of L17E (Figure 1A, route ii) was not so high as had been expected, and it facilitates cell permeation of cargoes at very early stages of endocytosis (Figure 1A, route i).[14] To achieve more effective pH-sensitive lytic activity for endosomal membranes, we focused on Glu and His residues within L17E. As described above, Glu may not be fully protonated, retaining a certain extent of negative charges at endosomal pH. Substitution of Glu to 2-aminoadipic acid (Aad, pK_a 4.21)[15,16] may be more favorable for endosomolysis due to the less charged feature of Aad at endosomal pH. His (pK_a ~6.0)[15] does not have charges at neutral pH, but it should be protonated and positively charged at endosomal pH, which may increase the hydrophilicity of the

peptide, diminishing its endosomolytic activity. Cellular uptake studies revealed that both His-to-Ala and Glu-to-Aad substitution worked favorably for enhancing the cytosolic delivery. Studies using endocytic inhibitors and physicochemical analysis using liposomes supports the effectiveness of these substitutions to facilitate the endosomal escape of the cargo molecules. When these substitutions are combined, a peptide named HAad was developed (Figure 1B), which attained cytosolic distribution of IgG and 10 kDa dextran in ~75% of cells in 60 min, while L17E attained distribution only in ~50% of the cells.The higher activity of HAad was also exemplified by recognizing nuclear pore complexes (NPC) using a delivered monoclonal antibody and by Cre recombinase activity. The potential *in vivo* application of this peptide was exemplified through the cerebral ventricle injection of Cre recombinase into the ventricle of Green Red Reporter (GRR) mouse together with HAad.

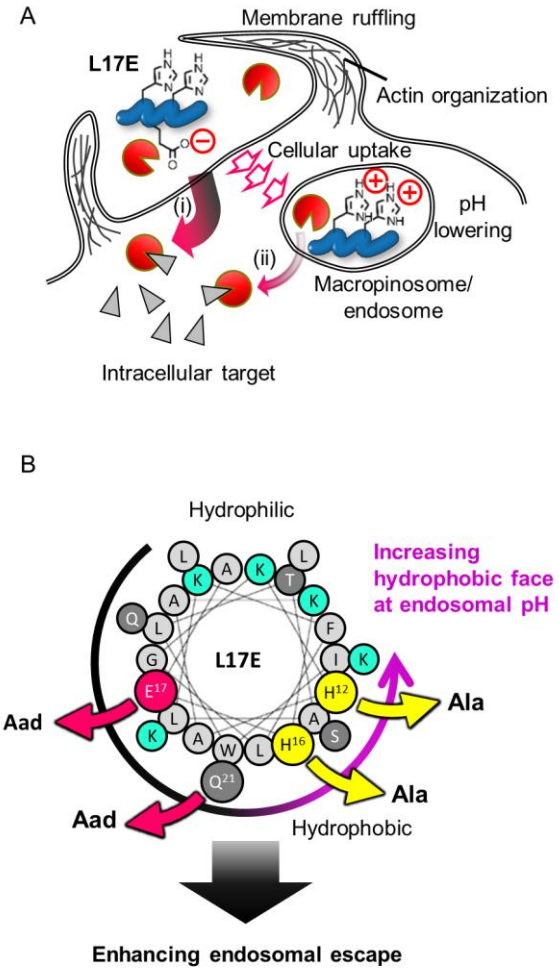

Figure 1. (A) Schematic representation of the mode of intracellular delivery by L17E. L17E was found to have an ability to induce membrane ruffling, leading to transient permeabilization of membranes at early stages of endocytosis and cytosolic translocation of biomacromolecules (route (i)). However, endosomal escape (route (ii)) did not play a significant role in attaining cytosolic translocation.[14] (B) Helical wheel projection of L17E showing substitutions of His^{12} and His^{16} to Ala, and Glu^{17} and Gln^{21} to Aad (=aminoadipic acid) resulting to HAad. Substitutions should lead to the enlargement of the potential hydrophobic face in endosomes and enhanced delivery using both routes (i) and (ii).

Results and Discussion

Amino acid substitution for facilitating endosomal escape

(i) Effect of substitution of Glu to 2-aminoadipic acid (Aad)

Figure 1B represents the helical wheel projection of L17E. Glu at position 17 (given in magenta in Figure 1B) is in the potential hydrophobic face of the peptide. Placement of Glu at this position effectively diminished the cytotoxicity of the original peptide M-lycotoxin (EC_{50} ~1.4 μM), and successfully converted the toxic lytic peptide to intracellular delivery tool with low toxicity (EC_{50} >40 μM).[13] In our previous work, L17D had lower cytosolic macromolecule-delivering activity than L17E.[13] Lower pK_a of β-COOH in Asp (3.90) compared to that of the γ-COOH in Glu (4.07)[15] should yield a higher population of charged form at endosomal pH, leading to the decrease in the hydrophobicity, the membrane interaction and the delivery activity of L17D compared with L17E (Figure 2A and B). L-2-aminoadipic acid (Aad) has a higher hydrophobicity compared with Glu and a higher pK_a of δ-COOH (4.21).[15,16] Substitution of Glu to Aad may thus work favorably for perturbation of endosomal membranes to allow endosomal escape. Dextran (10 kDa) labeled with Alexa Fluor 488 (Dex10-Alexa) was used as a model biomacromolecule. The ability for cytosolic delivery was evaluated using confocal laser scanning microscopy (CLSM) after incubation of HeLa cells with Dex10-Alexa in the presence of the peptide for 1 h (Figure 2C). Successful cytosolic delivery of Dex10-Alexa by the peptide should yield a uniform distribution and the diffuse signals of Dex10-Alexa throughout the cells. This was observed for ~50% cells by the treatment in the presence of 40 μM L17E and ~25% for 40 μM L17D, respectively, as previously reported (Figure 2C and D, L17E, L17D).[13] Notably, the cellular treatment with 40 μM L17Aad for 1 h yielded diffuse cytosolic labeling of Dex10-Alexa in 65% of the cells, i.e., 15% higher than L17E (Figure 2C and D, L17Aad). On the other hand, incubation of the cells with Dex10-Alexa in the absence of peptides yielded predominantly dot-like, punctate signals, suggesting endosomal entrapment of Dex10-Alexa with no substantial endosomal escape (Figure 2C and D, no peptide).

(ii) Effect of His-to-Ala substitution

The above results suggest the potential importance of increasing hydrophobicity of the peptides at endosomal pH on the stimulation of cytosolic Dex10-Alexa delivery. L17E contains two histidines (pK_a ~6.0)[15] (Figure 1B). These histidines are protonated or positively charged at endosomal pH, which may decrease the hydrophobicity and the membrane interaction of the peptide. The substitution of histidines to neutral amino acids may result in an increase of the endosomolytic activity. These histidines were thus substituted to alanines bearing methyl group (i.e., non-charged) for the side chain (HA/E1, Figure 3A and B). Alanine tends to favor α-helical structural formation, which may also increase the hydrophobic interaction with membranes and membrane lysis of the peptides (Figure 1B). The ability of peptides to facilitate cytosolic delivery was evaluated using Dex10-Alexa, as in the previous section.

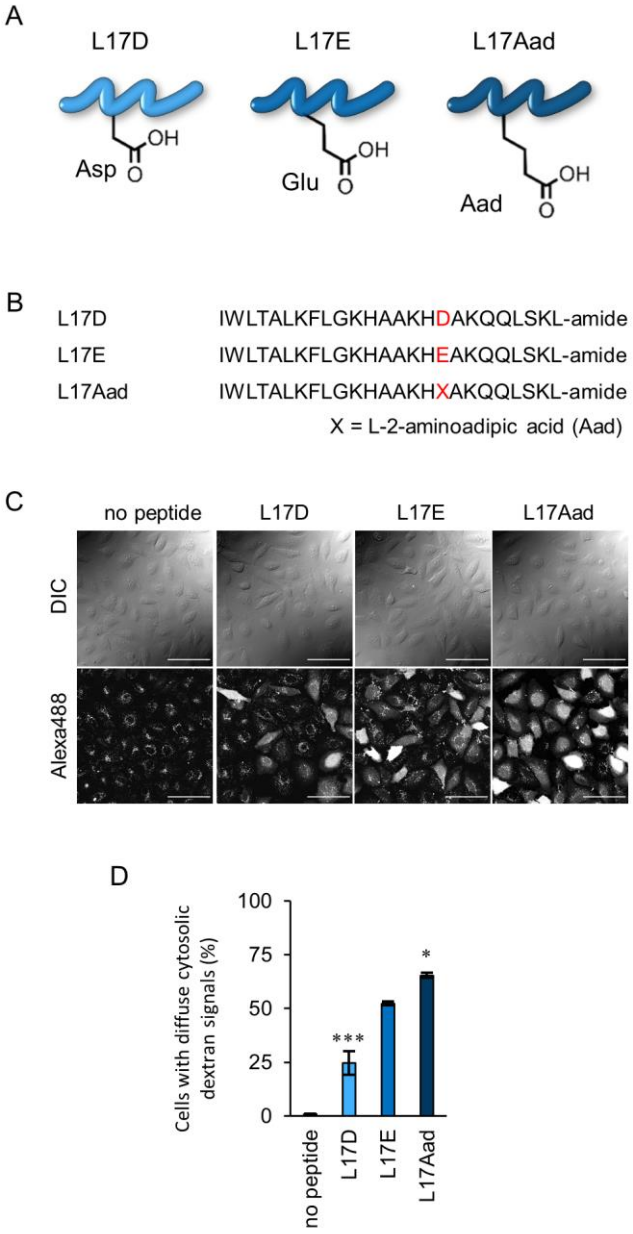

Figure 2. Effect of Glu[17] substitution of L17E on cytosolic delivery activity. (A) Schematic representation of L17E and its analogs. (B) Sequences of peptides. (C) Cytosolic appearance of Dex10-Alexa after treatment with L17E and its analogs (40 μM each) for 1 h. Scale bar, 100 μm. (D) Percentages of cells bearing diffuse cytosolic dextran signals. Results are presented as mean ± standard error (SE) (n = 3). *; p<0.05, ***; p<0.001 v.s. L17E (one-way analysis of variance (ANOVA) followed by Dunnett's post hoc test).

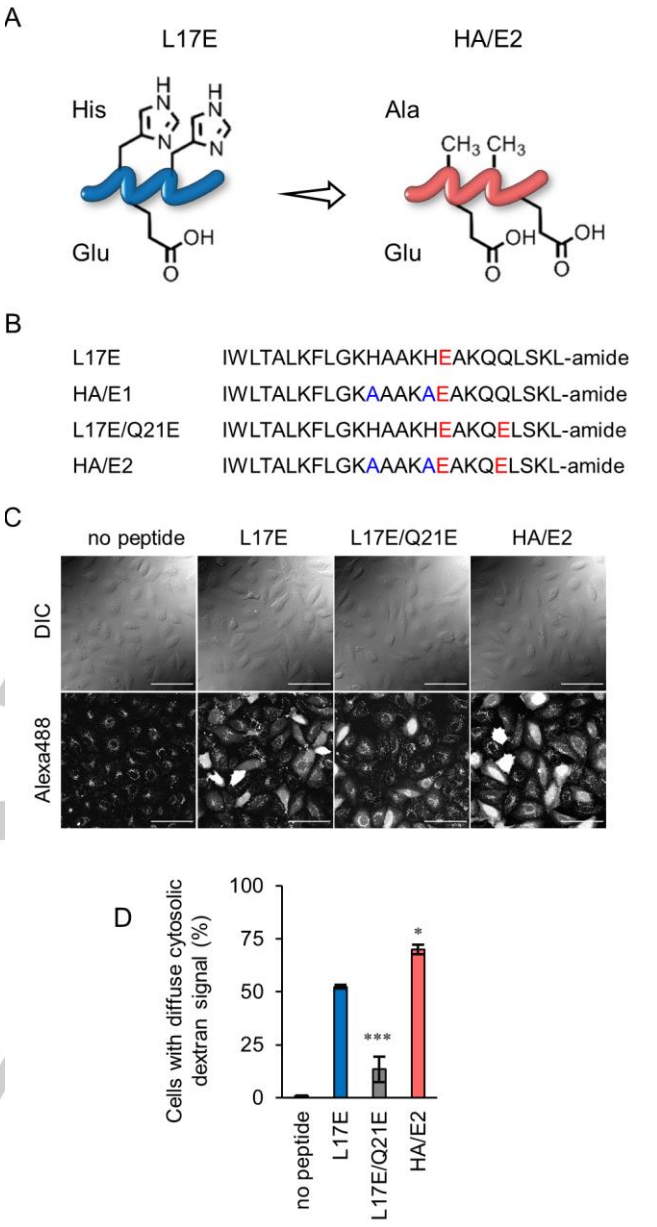

Figure 3. Improvement of cytosolic delivery efficacy of L17E by His-to-Ala substitution. (A) Outline of sequence modification. (B) Sequences of peptides bearing His-to-Ala substitutions. (C) The cytosolic appearance of Dex10-Alexa after treatment with L17E and its analogs (40 μM each) for 1 h. Scale bar, 100 μm. (D) Percentages of cells bearing diffuse cytosolic dextran signals. Results are presented as mean ± SE (n = 3). *; p<0.05, ***; p<0.001 vs. L17E (one-way analysis of variance (ANOVA) followed by Dunnett's post hoc test).

Compared with L17E yielding cytosolic Dex10-Alexa signal for ~50% cells, the same treatment using HA/E1, unfortunately, yielded considerable cell death (data not shown). Analysis by WST-8 assay (a mitochondrial dehydrogenase activity-based assay),[17] speculated that the His-to-Ala substitution yielded an excess increase in the hydrophobicity of the peptide, resulting in cell death. We, therefore, designed another analog HA/E2 (Figure 3A and B), which was similarly converted from L17E/Q21E peptide, having a slightly lower hydrophobicity and delivery efficacy next to L17E (yielding diffuse cytosolic Dex10-Alexa signal in ~30% of cells) in our previous paper.[13] Notably, treatment with HA/E2 yielded cytosolic Dex10-Alexa signal in ~70% of cells with no accompanied cytotoxicity (Figure 3C, D, and

S1). This number is significantly higher than that obtained by L17E. The above His-to-Ala substitution enlarged the potential hydrophobic face of L17E (Figure 1B). This may also lead to the enhancement of the hydrophobic interaction and membrane perturbation ability of the peptide, resulting in greater promotion of the endosomal release of Dex10-Alexa. Despite the use of His-containing peptides to stimulate endosomal escape by increasing osmotic pressure (i.e., via proton sponge effect) has been suggested,[18,19] this strategy requires a high number of histidine residues to achieve the desired effect.[20] L17E has two histidine residues only in its sequence, which may not be enough to elicit such effect.

(iii) High efficacy delivery attained through the combination of the above two substitutions

Finally, we combined all the above beneficial changes on L17E and came up with a new peptide, HAad (Figure 4A and B). About 75% of cells treated with 40 μM HAad and Dex10-Alexa showed cytosolic dextran signal (Figure 4C and D), and these results were even higher than those obtained with HA/E2 (Figure 3C and D), suggesting that HAad is the most effective among L17E analogs. Moreover, the number of cells yielding cytosolic signals upon treatment with 20 μM of HAad is comparable to that with 40 μM of L17E, suggesting that the efficiency of HAad is twice of L17E (Figure 4D). The total cellular uptake amount of Dex10-Alexa by the HAad treatment, analyzed by flow cytometry, was also ~30% higher than that by the L17E treatment (Figure 4E). No significant cytotoxicity accompanied this treatment (WST-8 assay, Figure S1).

HAad shares a similar mechanism with L17E to induce actin polymerization and membrane ruffling, allowing Dex10-Alexa to influx into cells via transient membrane perturbation of the ruffled membranes or at the early stage of endocytosis (Figure S2A). Note that as reported for L17E,[14] the translocation of Dex10-Alexa should not be attained by a simple pore formation in cell membranes by HAad and we therefore consider the method of permeabilization via membrane ruffling as a novel concept in intracellular delivery. Inhibition of Dex10-Alexa uptake by the treatment with 5-(*N*-ethyl-*N*-isopropyl)amiloride (EIPA), an inhibitor of membrane ruffling following Na^+/H^+ exchanger[21] was also observed (Figure S2B). A time-course experiment showed that 5 min was enough to deliver dextran to 50% of the cells for both L17E and HAad peptides (Figure 4F). On the contrary, no further increase in delivery for L17E treatment in prolonged incubation, while HAad further increased the uptake by 25%. These results suggested higher endosome perturbing activity of HAad than L17E. Interestingly, despite HAad attaining highly efficient cytosolic translocation of Dex10-Alexa, this peptide seems to be retained in endosomes or with endosomal membranes, judged by the CLSM analysis of the cells treated with C-terminally Alexa Fluor 488 labeled HAad [HAad-G_4C(Alexa488)] for 1 h (Figure S3). This observation may be due to the potential hydrophobic feature of HAad to favorably interact with membranes, allowing cytosolic translocation of the cargos.

HAad has an enhanced endosomal perturbation ability

The membrane perturbation ability of the peptides was analyzed by liposomal leakage assay (Figure 5A). Large unilamellar vesicles (LUVs, 200 nm diameter) containing 8-aminonaphthalene-1,3,6-trisulfonic acid (ANTS) as fluorophore and *p*-xylene-bis-pyridinium bromide (DPX) as quencher was

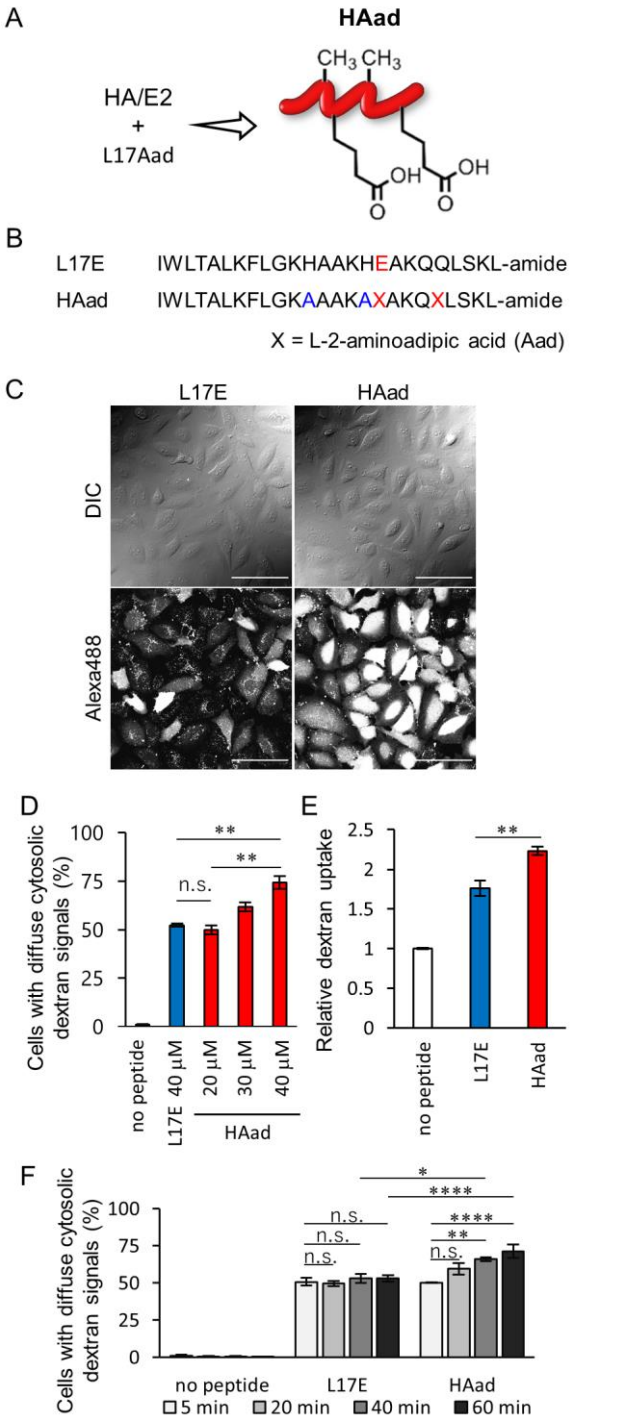

Figure 4. High efficacy cytosolic delivery peptide HAad. (A) Merged design of HA/E2 and L17Aad to obtain HAad. (B) Sequence of HAad. (C) High efficacy cytosolic delivery of Dex10-Alexa with the help of HAad (40 μM). Incubation, 1 h. Scale bar, 100 μm. (D) Percentages of cells bearing diffuse cytosolic dextran signals (incubation, 1 h). (E) Comparison of total cellular uptake amount of Dex10-Alexa by the incubation with each peptide (40 μM). (F) Time-dependent increase in the percentage of cells with diffuse cytosolic dextran signals by the treatment with L17E or HAad (40 μM each). Results are presented as mean ± SE (n = 3). ****; p<0.0001, **; p<0.01, *; p<0.05, n.s.; not significantly different by Tukey-Kramer's honestly-significant difference test (D, F) or Student's t-test (E).

employed.[22] Rupturing the liposomal membranes releases ANTS and DPX, leading to fluorescence recovery. The increase of resulting fluorescence is measured to observe the membrane perturbation tendency of the peptides. LUVs simulating the plasma membrane is composed of 1-palmitoyl-2-oleoyl-*sn*-glycero-3-phosphocholine (POPC). Reports state that late endosomes are abundant in negatively charged lipids, such as bis(monoacylgrycelo)phosphate (BMP).[23,24] Considering this point, a mixture of POPC and a negatively charged lipid 1-palmitoyl-2-oleoyl-*sn*-glycero-3-phosphoglycerol (POPG) (3:1) was employed to simulate endosomal membranes. Furthermore, neutral (7.4) and acidic pHs (5.0) are also used to replicate the extracellular and intra-endosomal pH, respectively.

As reported, L17E showed little leakage for POPC LUVs either at pH 7.4 or 5.0 at the P/L ratio between 10^{-4} and 1 (Figure 5A, left panel). On the other hand, a significant increase of fluorescence intensity, representing the leakage of dyes through the perturbed membrane, were observed from POPC/POPG LUVs treated with L17E at the P/L ratio of ~10^{-2} without pH preference. This finding confirms that L17E activity is predominantly related to lipid charge rather than on pH difference.[13] On the other hand, HAad had more significant perturbation activity for POPC/POPG LUVs at pH 5.0 than L17E, but the lower activity at pH 7.4 (Figure 5A, right panel). Considering that HAad had little effect on POPC LUVs at 7.4, this peptide may have a higher preference for endosomal membranes over cell membranes.

Circular dichroism (CD) study to analyze the secondary structure of the peptides also supports the broader pH switch of HAad in POPC/POPG LUVs at pH 5.0 over POPC LUVs at 7.4 (Figure 5B, left panel). Molar ellipticity at 222 nm ($[\theta]_{222}$) is a measure of the helical content of peptides.[25] L17E yielded only a marginal helical structure for POPC/POPG LUVs at both pHs ($[\theta]_{222}$ = –6.1 × 10^3 deg·cm^2/dmol at pH 7.4 and –6.4 × 10^3 deg·cm^2/dmol at pH 5.0, respectively). On the other hand, $[\theta]_{222}$ for HAad in the presence of POPC/POPG LUVs at pH 5.0 and that in the presence of POPC LUVs at 7.4 were –2.7 × 10^4 and –2.7 × 10^3 deg·cm^2/dmol, respectively, indicating the correlation of the leakage efficacy with helical content of these peptides.

To obtain information on the membrane-binding affinity of L17E and HAad, we also conducted tryptophan-binding assay under the same lipid concentration and P/L ratio with CD analysis (Figure S4). Both L17E and HAad have a tryptophan at the second residue from their N-terminus. The binding of the peptides to the lipid should result in a blue shift to ~330 nm, accompanied by an increase in fluorescence intensity (excitation at 280 nm).[26] L17E and HAad yielded a similar blue shift in the presence of POPC/POPG LUVs at pH 5.0 and 7.4, suggesting the binding of both peptides to negatively charged membranes. Minimal shifting was observed in the presence of POPC LUVs at either pH, suggesting weak binding of these peptides to the neutral membranes. Considering that both L17E and HAad bind with negatively charged membranes, these results suggested that increased hydrophobicity of HAad stimulating helical structural formation allowed the peptide to perturb negatively charged membranes at pH 5.0 better than L17E. These results could also explain the ability of HAad to allow higher cytosolic Dex10-Alexa transport at later stages in endosomal maturation.

Histidines in L17E are located at the border of potential hydrophobic/hydrophilic face in helical structure (Figure S5). The

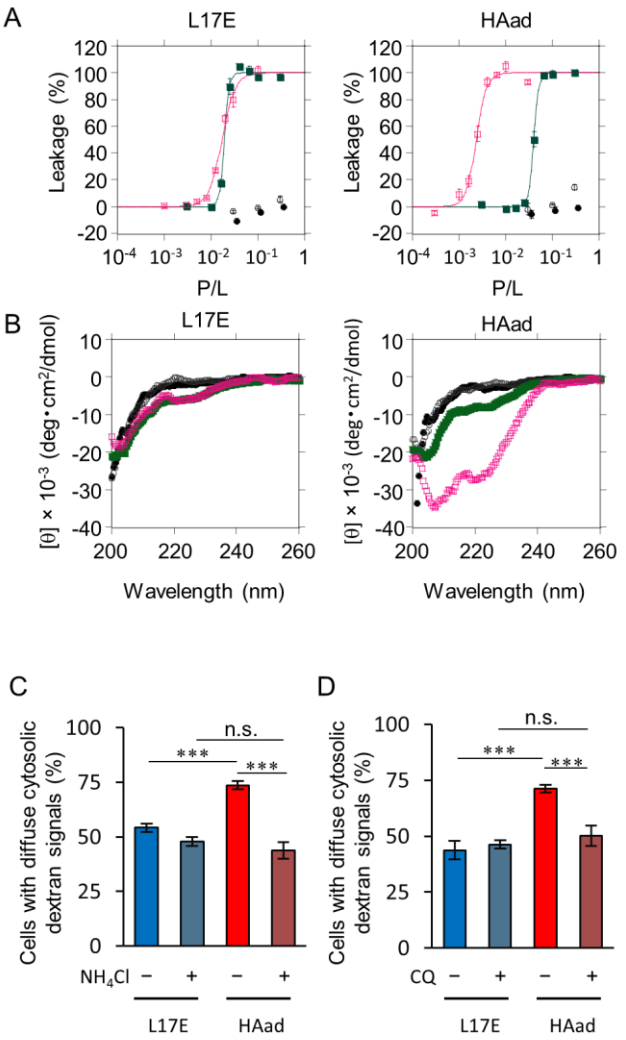

Figure 5. (A) Liposomal dye leakage by the treatment with L17E and HAad and (B) CD spectra of these peptides. Open magenta square, POPC/POPG (3:1) LUV at pH 5.0; filled green square, POPC/POPG (3:1) LUV at pH 7.4; open circle, POPC LUV at pH 5.0; filled circle, POPC LUV at pH 7.4. Effects of (C) NH4Cl and (D) chloroquine (CQ) on the percentages of cells having diffuse cytosolic Dex10-Alexa signals. Results are presented as mean ± SE (n = 3). ***; p<0.001, n.s.; not significantly different (one-way analysis of variance (ANOVA) followed by Tukey-Kramer's honestly-significant difference test). The results of liposomal leakage assay and CD analysis of HA/E2 and L17Aad are also given in Figure S6.

generation of positive charges may be favorable for the interaction of negatively charged lipid heads of endosomal membranes. However, charges in His may prevent the peptide from binding deep within the membrane via helical structure formation. The His-to-Ala substitution leads to increased hydrophobic area. This may enhance the peptide-membrane interaction to perturb the membranes while forming the helical structure.

Inhibitors and biological assays using galectin-8 confirmed the contribution of endosome maturation to the HAad-mediated cytosolic delivery. Treating cells with NH_4Cl and chloroquine

prevents endosome acidification.[27] No significant effect was observed in L17E treatment, while HAad-treated cells were negatively affected by the presence of these inhibitors (Figure 5C and D). This supports the need for endosomal maturation for HAad to attain additional cytosolic delivery compared to L17E. Disruption of endosomal membranes by HAad was also suggested by the study using galectin-8. Galectin-8 is a β-galactoside-binding protein.[28] Breaks on endosomal membranes allow galectin-8 to enter and bind to β-galactosides present inside endosomes.[29] Treatment of the cells expressing galectin-8 fused with an enhanced green fluorescent protein (EGFP) with HAad yielded dot-like punctate signals of galectin-8-EGFP in the cells (Figure S7, arrows), suggesting the rupture of endosomes. Efficient cytosolic Dex10-Alexa delivery by HAad was also observed in different cell lines (Figure S8). In our previous study, we found that L17E achieved efficient cytosolic translocation of Dex10-Alexa not only into human cervical carcinoma HeLa cells, but also human colon adenocarcinoma SW480 cells, African green monkey kidney fibroblast-like COS-7 cells, and human umbilical vein endothelial cells (HUVECs). However, the less efficient translocation was observed for mouse embryonic fibroblasts (NIH3T3).[13] HAad has improved cytosolic uptake into NIH3T3, yielding cytosolic Dex10-Alexa signals in ~40% of cells compared to ~20% with L17E. A similar effect was observed for human embryonic kidney HEK293 cells producing ~65% cytosolic Dex10-Alexa distribution using HAad but ~25% by L17E.

Cytosolic protein uptake activity of HAad

HAad has improved protein delivery over the previous design was confirmed through the delivery of antibodies (i.e., immunoglobulin Gs (IgGs)), EGFP bearing a nuclear localization signal, and Cre-recombinase. L17E has been reported to deliver IgG into cell interiors. Using IgG labeled with Alexa Fluor 488 (IgG-Alexa) (500 μg/mL), cytosolic delivery of IgG was attained in ~75% and ~50% of cells in the presence of HAad and L17E (40 μM each) in 1 h, respectively (Figure 6A). When the concentration of cargoes was decreased, we found that L17E was mostly effective at high IgG concentrations (higher than 200 μg/mL). HAad treatment was still effective until 50 μg/mL (~30%) (Figure 6B, Figure S9). This result could be due to the higher efficacy of HAad over L17E. Antigen recognition of delivered IgG was assessed through the delivery of Alexa Fluor 594 (Alexa594)-labeled anti-nucleopore complex (anti-NPC) IgG [anti-NPC IgG-Alexa594] (Figure 6C). Cells treated with 50 μg/mL anti-NPC IgG-Alexa594 in the presence of 40 μM HAad yielded the labeling of the nuclear periphery, while L17E produced a weaker signal due to its lower efficacy at this condition. The enhanced cytosolic protein delivery of HAad was also supported through the delivery of EGFP fused with a nuclear localization signal (NLS) derived from Simian Virus 40[30] (NLS-EGFP) (Figure S10). Evaluating the accumulation of EGFP signals in the nucleus may lead to a more precise evaluation of protein internalization than a simple analysis of cytosolic diffuse fluorescent signals. Notably, cotreatment with HAad resulted in around ~85% of cells having nuclear-localized NLS-EGFP signal, while L17E only achieved ~60%.

We further confirmed the delivery of functional proteins by HAad using a Cre-loxP recombination assay system (Figure 6D-F).[31] HeLa cells bearing *loxP-DsRed-STOP-loxP-EGFP* gene were treated with Cre recombinase (38 kDa, 5 or 10 μM) in the presence of HAad or L17E (40 μM each). Upon entry of Cre, site-

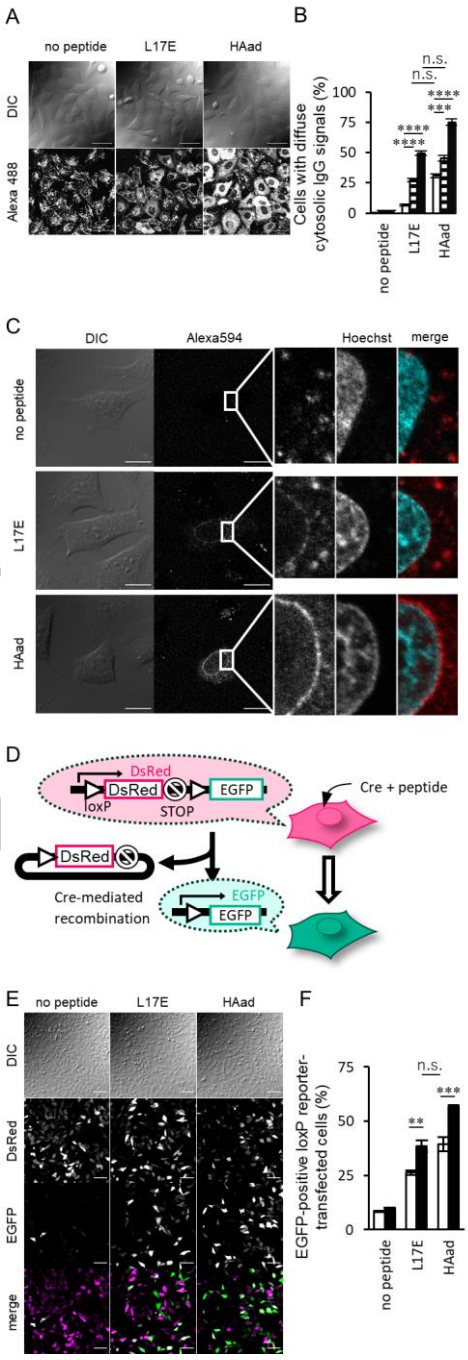

Figure 6. Superior ability of HAad in cytosolic cargo delivery. (A) Delivery of IgG-Alexa (500 μg/mL) in the presence of peptides. Scale bar, 50 μm. (B) Percentages of the cells having cytosolic IgG-Alexa signals. Open, hatched, and filled columns represent the incubation with 50, 200, and 500 μg/mL IgG-Alexa, respectively. (C) Localization of anti-NPC IgG-Alexa594 on nuclear membranes by the incubation with HAad. Scale bar, 20 μm. (D) Schematic representation of the Cre-loxP recombination assay system. (E) EGFP expression after the treatment with 10 μM Cre in the presence of 40 μM peptides. Scale bar, 100 μm. (F) EGFP-positive cells (%) in loxP reporter transfected cells. Open and filled columns represent the use of 5 and 10 μM Cre, respectively. Results are presented as mean ± SE (n = 3). ****; p<0.0001, ***; p<0.001, **; p<0.01, n.s.; not significantly different by Tukey-Kramer's honestly-significant difference test.

specific gene recombination is induced in reporter cells leading to the removal of the DNA segment expressing red fluorescent protein DsRed between the loxP sites and allowing expression of EGFP (Figure 6D). CLSM analysis suggests that incubation with 10 μM Cre in the presence of HAad resulted in ~60% of the total fluorescent protein-expressing cells (DsRed and EGFP) are showing EGFP (Figure 6E and F). With the same condition, L17E treatment only resulted in ~40% of cells having EGFP expression. This value was attained by HAad when half of the Cre amount (5 μM) in the presence (Figure 6F).

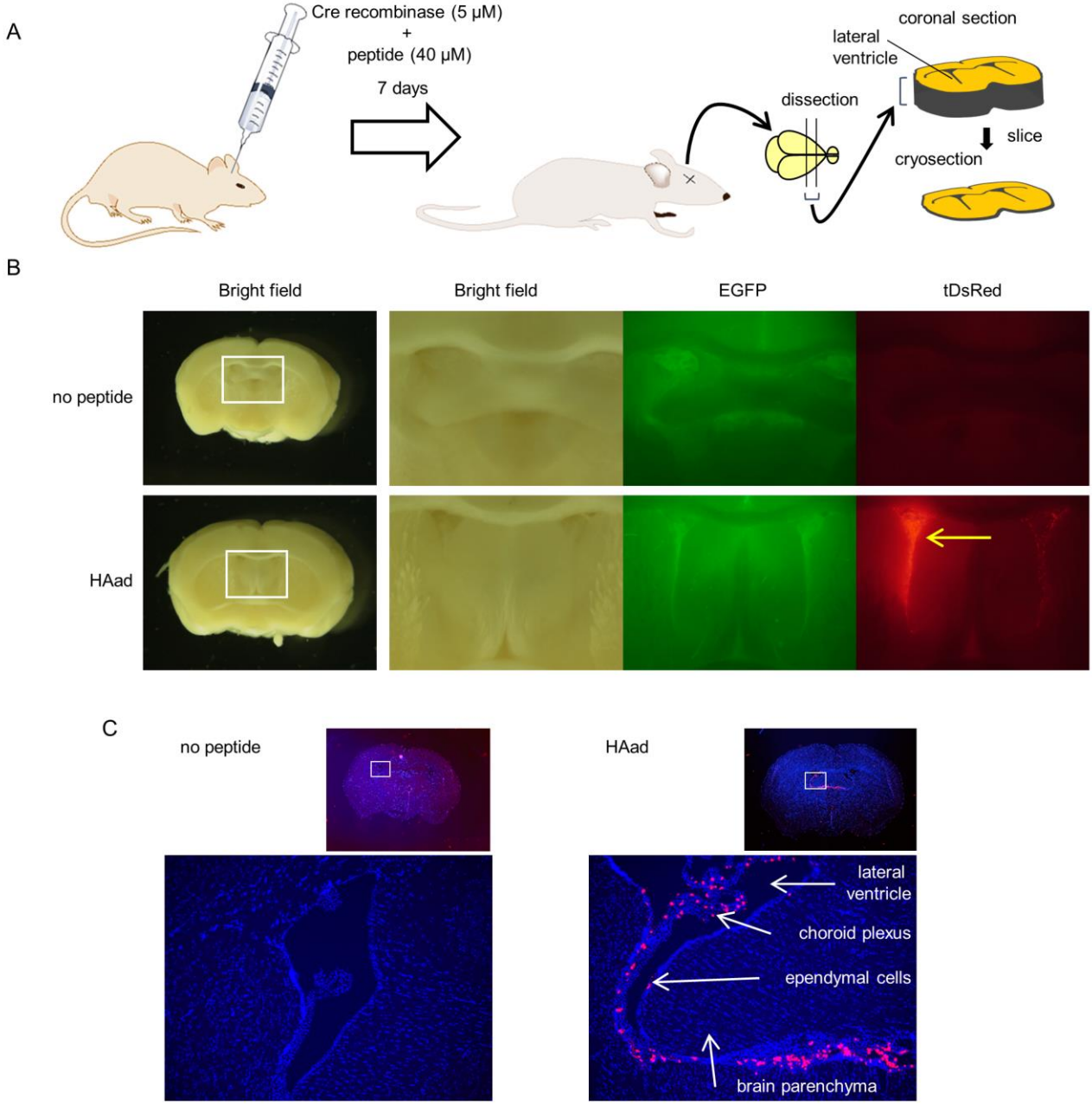

Figure 7. Peptide-mediated delivery (intracerebroventricular administration) of Cre recombinase into ependymal cells and choroid plexus faced to the lateral ventricle. (A) Schematic representation of Cre delivery into the brain. (B, C) Fluorescence images of the coronal section (B) and cryosection (C) of the brain. Right panels in (B) are enlarged images of the boxed areas in the left. Cre recombinase only (5 μM, "no peptide") or Cre recombinase and HAad (5 μM and 40 μM in 5 μL 0.9%NaCl, respectively) were injected into the right lateral ventricle. Expression of tDsRed, indicating the cytosolic delivery of Cre, were observed around the sites of injection with peptides (arrows). Lower panels in (C) represent enlarged pictures in the boxed areas in upper panels. Nuclei were stained with DAPI (blue). The tDsRed signals were predominantly observed at ependymal cells and choroid plexus, which face to lateral ventricle, whereas no significant signals were observed in brain parenchyma.

HAad–mediated delivery of Cre recombinase *in vivo*

To provide preliminary evidence on the potential application of HAad for *in vivo* cytosolic delivery of bioactive proteins, intracerebroventricular (i.c.v.) administration of Cre (used here as a model cargo protein) with HAad was performed on Cre-reporter knock-in mice R266GRR.[32] In this mouse model, cytosolic delivery of Cre leads to EGFP-to-tDsRed change in fluorescence, allowing spatiotemporal observation of Cre recombination accomplished in each Cre-driver mouse strain. The cerebral ventricles are interconnected cavities of the brain filled by cerebrospinal fluid and the site for i.c.v. administration and a potential route for drug delivery into brain.[33] Cre recombinase and HAad were injected into the cerebral ventricle in R26GRR mice. Seven days after i.c.v. administration, anesthetized mice were perfused with paraformaldehyde in phosphate-buffered saline (PBS), and brains were dissected at the coronal section (Figure 7A). Figure 7B represents fluorescence images of the coronal section. Although expression of EGFP (green) was observed in the whole section, significant red signals, indicating the expression of tDsRed (red) were observed around the sites of Cre injection (right lateral ventricle in the cerebral ventricle) following the cytosolic delivery of Cre together with HAad (arrows in Figure 7B). Figure 7C represents the cryosection images with 4´,6-diamino-2-phenylindole (DAPI)-stained nuclei (indicating localization of the cells in the brain). The overlap of the tDsRed (red) and DAPI (blue) signals represent cells showing gene recombination after internalization of Cre with the help of HAad. This was predominantly observed in ependymal cells (cells lining the cerebral ventricle) and choroid plexus (localized in the cerebral ventricle and involved in producing the cerebrospinal fluid), which face to lateral ventricle, suggesting that HAad can be applied for protein delivery *in vivo*. Additionally, no significant tDsRed signals were observed in brain parenchyma or in the absence of peptides, suggesting the need for further improvements for this peptide to be applicable as a delivery system for cells located deep within tissues.

Conclusion

Helical structure formation at endosome conditions increases hydrophobic interaction with and rupture of endosomal membranes. Considering this, we designed HAad having Glu/Gln-to-Aad and His-to-Ala substitutions and showed its superiority over its predecessor. From a endosomolytic peptide design point-of-view, this study provided two lessons: 1) the difference of a single methylene moiety in the side chains observed between L17E and L17Aad, accompanied by a slight increase in pK_a and the hydrophobicity, yielded better delivery activity, and 2) While the histidine residues have been considered to bestow “proton sponge effect”, bursting endosomes, increment in hydrophobicity in endosomal milieu by the His-to-Ala substitution seems to work favorably when the numbers of His in the endosomolytic peptides are limited. The resulting HAad showed a greater extent of unstructured-to-helix transition and membrane perturbation at endosome-mimicking condition (i.e., LUVs containing negatively charged lipids at pH 5.0) over the cell membrane-mimicking condition (i.e., LUVs composed of neutral, zwitterionic lipids at pH 7.4). Despite both HAad and L17E mediating cytosolic delivery at the early stage of endocytosis, HAad more efficiently delivered cargo proteins into cytosol due to its enhanced endosomolytic activity. This peptide generally attains cytosolic delivery of dextran and proteins at 1.5-fold cells higher than L17E. Also, HAad resulted in similar levels of Cre recombination activity using half the amount of cargo protein than L17E. Uptake in different cell lines also supports the generality of HAad. These improvements were possible through the design focused on both the negatively charged feature of endosomal membranes and the well-recognized lowered pH in endosomal compartments. Arranging charges and hydrophobicity based on these features resulted in the creation of HAad. HAad retained the mechanisms of L17E, i.e., induction of membrane ruffling and transient membrane perturbation at the early stage of endocytosis to allow cytosolic translocation of the cargo molecules. Therefore, using both the physiological stimulation (i.e., membrane ruffling) and improved physicochemical features (i.e., preferential perturbation of negatively charged membranes at acidic pH), HAad achieved high efficacy of cytosolic protein delivery.

Acknowledgements

This work was supported by JSPS KAKENHI (Grant Numbers 18H04403 and 18H04017), and by JST CREST (Grant Number JPMJCR18H5). K.S. and M.A. are grateful for the JSPS Research Fellowship for Young Scientists.

The authors declare no competing financial interest.

Keywords: cytosolic protein delivery; amphiphilic cationic lytic peptide; histidine; aminoadipic acid; in vivo delivery

[1] S. Guillard, R. R. Minter, R. H. Jackson, *Trends Biotechnol.* **2015**, *33*, 163–171.
[2] K. Singh, W. Ejaz, K. Dutta, S. Thayumanavan, *Bioconjug. Chem.* **2019**, *30*, 1028–1041.
[3] P. D. Kaiser, J. Maier, B. Traenkle, F. Emele, U. Rothbauer, *Biochim. Biophys. Acta* **2014**, *1844*, 1933–1942.
[4] S. A. Smith, L. I. Selby, A. P. R. Johnston, G. K. Such, *Bioconjug. Chem.* **2019**, *30*, 263–272.
[5] D. Pei, M. Buyanova, *Bioconjug. Chem.* **2019**, *30*, 273–283.
[6] D. J. Brock, H. M. Kondow-Mcconaghy, E. C. Hager, J. P. Pellois, *Bioconjug. Chem.* **2019**, *30*, 293–304.
[7] A. El-Sayed, S. Futaki, H. Harashima, *AAPS J.* **2009**, *11*, 13–22.
[8] W. Li, F. Nicol, F. C. Szoka, *Adv. Drug Deliv. Rev.* **2004**, *56*, 967–985.
[9] A. Erazo-Oliveras, K. Najjar, L. Dayani, T. Y. Wang, G. A. Johnson, J. P. Pellois, *Nat. Methods* **2014**, *11*, 861–867.
[10] L. D. Mayer, M. J. Hope, P. R. Cullis, *Biochim. Biophys. Acta* **1986**, *858*, 161–168.
[11] S. Kim, S. Hyun, Y. Lee, Y. Lee, J. Yu, *Biomacromolecules* **2016**, *17*, 3007–3015.
[12] M. Li, Y. Tao, Y. Shu, J. R. LaRochelle, A. Steinauer, D. Thompson, A. Schepartz, Z. Y. Chen, D. R. Liu, *J. Am. Chem. Soc.* **2015**, *137*, 14084–14093.
[13] M. Akishiba, T. Takeuchi, Y. Kawaguchi, K. Sakamoto, H.-H. Yu, I. Nakase, T. Takatani-Nakase, F. Madani, A. Gräslund, S. Futaki, *Nat. Chem.* **2017**, *9*, 751-761.
[14] M. Akishiba, S. Futaki, *Mol. Pharm.* **2019**, *16*, 2540–2548.
[15] W. H. E. and K. M. J. Rex M. C. Dawson, Daphne C. Elliott, *Data for Biochemical Research*, Oxford Science Press, **1986**.
[16] S. Kim, S. Hyun, Y. Lee, Y. Lee, J. Yu, *Biomacromolecules* **2016**, *17*, 3007–3015.
[17] M. Ishiyama, Y. Miyazono, K. Sasamoto, Y. Ohkura, K. Ueno, *Talanta* **1997**, *44*, 1299–1305.
[18] Y. W. Cho, J.-D. Kim, K. Park, *J. Pharm. Pharmacol.* **2003**, *55*, 721–734.

[19] T. Iwasaki, Y. Tokuda, A. Kotake, H. Okada, S. Takeda, T. Kawano, Y. Nakayama, *J. Control. Release* **2015**, *210*, 115–124.
[20] J. Shi, J. G. Schellinger, R. N. Johnson, J. L. Choi, B. Chou, E. L. Anghel, S. H. Pun, *Biomacromolecules* **2013**, *14*, 1961–1970.
[21] O. Meier, K. Boucke, S. V. Hammer, S. Keller, R. P. Stidwill, S. Hemmi, U. F. Greber, *J. Cell Biol.* **2002**, *158*, 1119–1131.
[22] H. Ellens, J. Bentz, F. C. Szoka, *Biochemistry* **1984**, *23*, 1532–1538.
[23] T. Kobayashi, E. Stang, K. S. Fang, P. De Moerloose, R. G. Parton, J. Gruenberg, *Nature* **1998**, *392*, 193–197.
[24] H. Matsuo, J. Chevallier, N. Mayran, I. Le Blanc, C. Ferguson, J. Fauré, N. S. Blanc, S. Matile, J. Dubochet, R. Sadoul, et al., *Science* **2004**, *303*, 531–534.
[25] R. W. Woody, *Methods Enzymol.* **1995**, *246*, 34–71.
[26] K. Matsuzaki, O. Murase, H. Tokuda, S. Funakoshi, N. Fujii, K. Miyajima, *Biochemistry* **1994**, *33*, 3342–3349.
[27] B. Poole, S. Ohkuma, *J. Cell Biol.* **1981**, *90*, 665–669.
[28] D. A. and Y. Z. Yaron R. Hadari, Keren Paz, Roi Dekel, Tomislav Mestrovic, *jounal Biochem. Chem.* **1995**, *270*, 3447–3453.
[29] K. V. Kilchrist, S. C. Dimobi, M. A. Jackson, B. C. Evans, T. A. Werfel, E. A. Dailing, S. K. Bedingfield, I. B. Kelly, C. L. Duvall, *ACS Nano* **2019**, *13*, 1136–1152.
[30] D. Kalderon, B. L. Roberts, W. D. Richardson, A. E. Smith, *Cell* **1984**, *39*, 499–509.
[31] K. Araki, M. Araki, J. I. Miyazaki, P. Vassalli, *Proc. Natl. Acad. Sci. U. S. A.* **1995**, *92*, 160–164.
[32] Y. Hasegawa, Y. Daitoku, K. Sekiguchi, Y. Tanimoto, S. Mizuno-Iijima, S. Mizuno, N. Kajiwara, M. Ema, Y. Miwa, K. Mekada, et al., *Exp. Anim.* **2013**, *62*, 295–304.
[33] J. L. Cohen-Pfeffer, S. Gururangan, T. Lester, D. A. Lim, A. J. Shaywitz, M. Westphal, I. Slavc, *Pediatr. Neurol.* **2017**, *67*, 23–35.

Entry for the Table of Contents

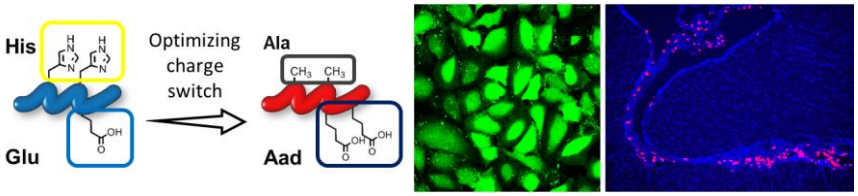

An endosomolytic peptide HAad was developed for the efficient intracellular delivery of biomacromolecules. Notable design features include (i) using aminoadipic acid (Aad) as a safety-catch for preferential permeabilization of endosomal membrane over the cell membrane, and (ii) His-to-Ala substitutions to enhance endosomolytic activity. HAad attained successful delivery of functional proteins *in vitro* cell cultures and *in vivo* mouse brain.